

General Disclaimer

One or more of the Following Statements may affect this Document

- This document has been reproduced from the best copy furnished by the organizational source. It is being released in the interest of making available as much information as possible.
- This document may contain data, which exceeds the sheet parameters. It was furnished in this condition by the organizational source and is the best copy available.
- This document may contain tone-on-tone or color graphs, charts and/or pictures, which have been reproduced in black and white.
- This document is paginated as submitted by the original source.
- Portions of this document are not fully legible due to the historical nature of some of the material. However, it is the best reproduction available from the original submission.

University of Cincinnati, Cincinnati, Ohio 45221

NUMERICAL STUDY OF SUPERSONIC TURBULENT
FLOW OVER SMALL PROTUBERANCES

Semiannual Progress Report,
July - December 1975

NASA Grant No. NSG 1208

(NASA-CR-145924) NUMERICAL STUDY OF
SUPERSONIC TURBULENT FLOW OVER SMALL
PROTUBERANCES Semiannual Progress Report,
Jul. - Dec. 1975 (Cincinnati Univ.) 16 p HC
\$3.50

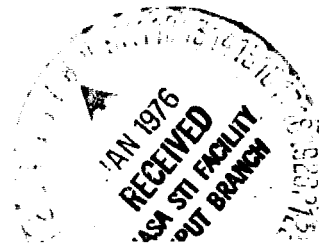
N76-14043

Unclas
06795

CSCL 20D G3/02

Principal Investigators are A. Polak and M. J. Werle,
Department of Aerospace Engineering.

The NASA Technical Officer for this grant is Mr. James
C. Dunavant, NASA Langley Research Center, Hampton,
Virginia 23665.



NUMERICAL STUDY OF SUPERSONIC TURBULENT
FLOW OVER SMALL PROTUBERANCES

NASA Grant No. NSG 1208

Semi-Annual Status Report
July 1, 1975 - December 31, 1975

by

A. Polak and M.J. Werle
University of Cincinnati, Cincinnati, Ohio

This report summarizes the effort expended during the first six months on the study of supersonic turbulent boundary layers over two-dimensional protuberances. The approach taken is to extend an earlier work (Ref. 1) to the turbulent regime, using the numerical finite-difference alternating direction implicit (ADI) method. An obvious departure from the previous case (Ref. 1) is forced by the need to model mathematically the turbulence. The turbulence is represented here by the eddy viscosity approach as used in Refs. (2) and (3). The turbulent boundary layer structure as well as an interest in thick boundary layers and much larger protuberance heights than in the laminar case lead to new difficulties. The problems encountered in the course of the present investigation and the means to remove them will be discussed later in this report.

The governing equations pertinent to the problem are

Continuity

$$V_{\eta} + F + 2\xi F_{\xi} = 0$$

Momentum

$$(\ell \bar{\epsilon} F_\eta)_\eta - V F_\eta + (1 + \alpha/2) \left(\beta + \frac{\partial \Delta_T}{\partial t} \right) (g - F^2) - 2 \xi F F_\xi = 0$$

Energy

$$\left(\frac{\ell \hat{\epsilon} g_\eta}{Pr} \right)_\eta - V g_\eta \frac{2\alpha}{2+\alpha} \left[\ell (\bar{\epsilon} - \hat{\epsilon} / Pr) F F_\eta \right]_\eta - 2 \xi F g_\xi = 0$$

with

$$F(\xi, 0) = V(\xi, 0) = 0, \quad g(\xi, 0) = H_w / H_e$$

$$F(\xi, \infty) = g(\xi, \infty) = 1.$$

This momentum equation is cast into the present form to facilitate the use of the ADI algorithm. The notation is the same as in Refs. (1) and (3). Hence, F = normalized streamwise component of velocity, g = normalized total enthalpy, V = transformed normal velocity function, Δ_T = total displacement body, ℓ = molecular viscosity parameter, α = an inviscid parameter, and $\bar{\epsilon}$ and $\hat{\epsilon}$ are eddy viscosity parameters defined for fully turbulent flow as $\bar{\epsilon} = 1 + \epsilon/\mu$, $\hat{\epsilon} = 1 + \frac{Pr}{Pr_T} \epsilon/\mu$, where ϵ = eddy viscosity. The Prandtl numbers, Pr and Pr_T are taken to be constant.

The study commenced with programming the above equations using the Cebeci-Smith two-layer eddy viscosity model, applied successfully to attached* turbulent boundary layers earlier (Refs. (2), (3)). A

* Initially, this choice is adequate since the immediate aim is to develop an efficient numerical algorithm; comparison with experimental data will be delayed for later.

base case was identified with flow conditions corresponding to the NASA test data (Ref. (4)). The free stream Mach number and static temperature are $M_\infty = 2.5$ and $T_\infty = 252^\circ\text{R}$ respectively. The Reynolds number based on free stream conditions and a reference length $L^* = 15.25$ cm is $Re_\infty = 1.647 \times 10^6$. The sine-wave protuberance profile is given by $y = \frac{h}{2} \{1 - \cos [\frac{2\pi}{w} (x - x_A)]\}$, where h is the height and w is the width of the protuberance. In all the base case studies $w = 0.24$ (i.e. $w^* = 0.24 \times 15.25$ cm = 3.66 cm; star quantities are dimensional). For a single wave placed on a flat plate far downstream from the leading edge, at $s = 25.85$, and $h = 0.02$ a calculation was performed with $T_w/T_o = 0.81$, $Pr = 0.72$ and $Pr_T = 0.9$. An attached solution was obtained (Fig. 1). In this case the boundary layer displacement thickness δ is about three times the protuberance height (but only about 1/3 as thick as the NASA Langley tunnel wall boundary layer). The calculation commenced at $s_i = 1.0$ with a laminar boundary layer, passing through transition and becoming fully turbulent at $s = 1.4$. After sweeping only once in ξ direction up to station $s_o = 25.5$ the ADI algorithm is employed between stations s_o and $s_f = 26.5$. The protuberance is placed between $x = 25.85$ and 26.09 . The stream-wise step size, Δs was taken 0.02 in this calculation so that there are at least 12 grid points over the protuberance surface. In 6.7 minutes of computer time 22 time sweeps were performed and the skin friction is varying (between the last two time steps at a given station) in the third or higher decimal place. This was considered a converged solution. It is worthwhile noticing that in the laminar case (Ref. 1) the same number of time steps required about 15-20 minutes computer time. The present efficiency was accomplished by linearization of the

coefficients of the corresponding difference equation around the previous station value, eliminating thus the need to update these coefficients in subsequent iterations.

Increasing the protuberance height at otherwise identical flow conditions as given above, a separation region appeared ahead of the protuberance. But the values of skin friction (the parameter we monitor for testing the quality of the solution) did not converge in time. On the contrary, wide oscillations occurred in time indicating some numerical instability, and eventually the calculation terminated abruptly. Examination of the boundary layer velocity profiles showed slight oscillations (of order 10^{-6} around the value $F = 1$) in the boundary layer edge region. At this point it was not clear whether this was due to a stronger interaction (higher protuberance), the reverse flow region, an improper eddy model or some other effects. To isolate the source of trouble it was decided to simplify the problem by taking $Pr = Pr_T = 1$, thus eliminating the need to solve the energy equation. (This corresponds to adiabatic wall condition with $g = \text{constant} = 1$); the rationale being that since the artificial time dependent term appears only in the momentum equation, the source of the time-like oscillations maybe due to finite-difference representation of this equation. Because the difficulty appeared for the separated cases, the eddy viscosity model became suspect as well. 'Freezing' the eddy viscosity distribution (this idea was borrowed from Ref. 5) near the forward plate-protuberance junction, and the use of Alber's model (Ref. 6) for the separated region did not resolve the difficulty. It was brought to our attention (Ref. 7) that upwind differencing of the F_{η} term in the momentum equation maybe required to satisfy the

convergence criteria of the numerical scheme (see also Ref. 8). In the present case the momentum equation, after linearization, may be written as

$$F_{\eta\eta} + \alpha_1 F_{\eta} + \alpha_2 F + \alpha_3 + \alpha_4 F_{\xi} + \alpha_5 V = 0 \quad ,$$

where $\alpha_1, \dots, \alpha_5$ are the linearized coefficients. In the boundary layer near the wall the diffusion term $F_{\eta\eta}$ is predominant over the convection-like term $\alpha_1 F_{\eta}$ and a central difference scheme for F_{η} is appropriate. From a so-called diagonal dominance test of the model equation $F_{\eta\eta} + \bar{\alpha} F_{\eta} = 0$ it is found that with central differencing the criteria $|\bar{\alpha}\Delta\eta| \leq 2$ must be met. Because of additional terms in the momentum equation we have found (by numerical experimentation) that the use of the criteria $|\bar{\alpha}\Delta\eta| \leq 1$ eliminated the oscillations in the profile near the boundary layer edge. Hence, F_{η} is central differenced when $|\bar{\alpha}\Delta\eta| \leq 1$ and upwind differencing is used when $|\bar{\alpha}\Delta\eta| > 1$. Davis (Ref. 7) also pointed out that the use of forward differencing of F_{ξ} term in the continuity equation is more appropriate because the upstream propagation becomes important for the strongly interacting boundary layers. Having incorporated these ideas into our algorithm difficulties mentioned above have been removed; the boundary layer profile approaches smoothly the edge values ($F = 1$) and the time-like oscillations also disappeared. For the base flow conditions, with the forward junction of the plate-protuberance placed at $s_A = 3.35$ and protuberance height of 0.024 results are shown in Figures 2 and 3. The dashed line in Figure 2 represents the variation of wall shear with time steps at a fixed station ($s = 3.33$) located just downstream of the plate-protuberance junction. This typically unstable solution, obtained before

the above mentioned changes were introduced, terminates abruptly after ten time steps. After the modifications in the numerical algorithm were made an apparently convergent solution was obtained (full line, Fig. 2). The variation in C_f appears only in the third or higher decimal place after the first fifteen time steps. The spatial distribution of C_f at the last time step (33rd sweep) is plotted in Figure 3. A small separation bubble appears near the forward plate-protuberance junction and the maximum shear is about double that of the flat plate value. The boundary layer displacement thickness ahead of the protuberance is relatively thin, $\delta \approx 0.010$ (or $\delta^* = \delta L^* = 0.1525$ cm) and $\delta/h = 0.4$.

A major interest of this research project is in comparisons of the numerical predictions with experimental data of very thick separated turbulent boundary layers produced on the tunnel wall (Ref. 4). The separation characteristics over the test plate placed in the wind tunnel wall are strongly dependent on the approaching turbulent boundary layer profile. For this reason calculations were performed for the boundary layer as it develops along the wall of the UPWT Langley Tunnel. The following test section free-stream conditions were taken: $M_\infty = 2.535$, $Re_\infty/cm = 1.08 \times 10^5$, $T_\infty = 567^\circ R$ ($315^\circ K$), $T_w = 252^\circ R$, $T_w/T_\infty = 0.81$, $Pr = 0.72$, $Pr_T = 0.9$. A reference length $L^* = 15.25$ cm ($= 0.5$ ft). Correspondingly, the reference Reynolds number is $Re = \frac{\rho_\infty^* u_\infty^* L_\infty^*}{\mu_\infty^*} = 1.08 \times 10^5 \times 15.25 = 1.647 \times 10^6$, and the nondimensional protuberance width w of 0.24 corresponds to w^* of 3.66 cm. The boundary layer calculation was carried out as a non-interacting 2-D laminar-transitional-turbulent boundary layer developing from ahead of the nozzle throat under a favorable pressure gradient. In the supersonic region downstream of the throat the pressure distribution was calculated from the sidewall

Mach number distribution, using isentropic relations. The Mach number distribution was obtained from a characteristic net (Ref. 9). From these data a cubic representation for M was assumed of the form

$$M = M_T - K_1 \left(1 - \frac{s}{s_T}\right)^2 \left(1 - K_2 \frac{s}{s_T}\right),$$

where M_T = test section Mach number at $s = s_T$. The above polynomial representation satisfies the condition $dM/ds = 0$ at $s = s_T$. At the location s_α of the first characteristic near the throat the Mach number was estimated to be $M_\alpha = 1.11$. The measured distance along the wall from s_α to s_T is 39.6 (\approx 20 ft). At a location s_β 8.86 units downstream of s_α the Mach number is $M_\beta = 1.84$. Letting $s_\alpha = 1$, $s_\beta = 9.86$ and $s_T = 40.6$. Using these values, the constants K_1 and K_2 can be determined. For $K_1, K_2 > 0$ and $K_2 \leq 1$ (which is the case here) the polynomial representation given above yields monotonically increasing Mach number. The subsonic-transonic section of the tunnel was also assumed to be represented by a cubic polynomial

$$M = M_i + C_1 \left(1 - \frac{s}{s_i}\right)^2 \left(1 - C_2 \frac{s}{s_i}\right),$$

with the following properties:

At $s = s_i = 0.3$, $M = M_i$ and $dM/ds = 0$.

At $s = s_\alpha$, $M = M_\alpha = 1.11$ and $\frac{dM}{ds} = \frac{dM}{ds} \Big|_{s_\alpha}$.

Three different values for M_i were chosen: 0.01, 0.03 and 0.05.

It turned out that the boundary layer development downstream of the throat was not sensitive to these initial values. Taking $M_i = 0.03$

a boundary layer calculation was performed for $0.3 \leq s \leq 97.4$ with nine complete boundary layer profiles punched on IBM cards between locations 40.6 and 72.6. (At $s = 40.6$ the Mach number becomes constant on the side wall; at $s \approx 50.6$ the straight section begins). These profiles are presently being used as initial data for separation studies of thick turbulent boundary layers. The table below gives the calculated boundary layer displacement thickness distribution along the constant Mach number section of the UPWT Langley tunnel wall at ten stations

s	40.6	44.6	48.6	52.6	56.6	60.6	64.6	68.6	72.6	76.6
δ^* (cm)	1.69	1.84	1.98	2.12	2.26	2.40	2.54	2.67	2.80	2.93

Using the profile produced at station $s = 72.60$ and placing a single sine-wave protuberance on the flat with its junction at $s_A = 73.25$ calculations were initiated to obtain separation characteristics of thick turbulent boundary layers. The calculation starts at $s = 72.60$ by sweeping once to station 72.96 and then the ADI algorithm was employed between this station and $s = 73.96$ using 51 grid points in the s direction ($\Delta s = 0.02$) with 105 point variable mesh in η direction. Figure 4 shows results obtained for the base case flow conditions with $h = 0.08$, $w = 0.24$, $Pr = 0.72$, $Pr_T = 0.90$ and $T_w/T_o = 0.81$. Note that here the energy equation was solved simultaneously with the continuity and momentum equations. Figure 4 shows the variation of the surface skin friction and pressure levels predicted by the present method. It is seen that ahead of the protuberance the skin friction drops and a small separation region develops on the front face of the wave. The

skin friction peaks just aft of the wave top with a value three times the undisturbed flat plate value. The pressure distribution is somewhat different and shows a monotonic increase up to a peak near the top of the wave followed by a mild recovery back to the flat plate value.

While the above results demonstrate the capability of the present method to handle flow fields typical of present interest, there remain several refinements to be made before the technique can be considered operational.

The first of these involves the size of the finite difference mesh applied to the problem. Using the present mesh from $s = 73$ to 74 it is noticed that the surface pressure distribution for all points in the mesh ahead of an aft of the protuberance is influenced by the protuberance. This effect is manifest by the depressed pressure levels ($p/p_\infty < 1$) near $s = 73$ and the monotonically increasing levels of \bar{C}_f ahead of protuberance. A test was conducted with the ends of the finite difference mesh moved away from the protuberance. This led to a relief of this difficulty. Apparently a larger number of grid points ahead of the protuberance will have to be used.

The second area of interest needing further study is the convergence rate of the iterative scheme. The present ADI numerical algorithm is conditionally stable and the convergence rate sensitive to the time step chosen. For the solutions depicted in Figure 4, convergence was achieved in about 40 iterations (approximately 10 minutes) and this computer time can be further reduced by either reducing the number of grid points (presently set at 5000) or parametrically assessing the optimum value of Δt . Through these two efforts it would be anticipated

that the computer effort could be reduced to the 2 or 3 minute level. Efforts in this direction will be made during the second half of this study.

Another point of interest involves the sensitivity of the present solution method to the initialization procedure. At present the solution method is found to show some influence of initial conditions (time = 0) on the final steady state values, mainly in the separated region and the source of this anomaly is presently not known. This problem could be due to either a programming error (a possibility now being investigated) or a conceptual error. It is possible that the influence of the confined finite difference mesh discussed above is causing this problem, but it is not yet clear how this would occur. Another possibility is that the consistency error of the ADI scheme (Ref. 10) is producing this difference and this possibility will also be considered.

Following this an eddy viscosity model which is more appropriate for separated boundary layers will be incorporated into the algorithm before comparisons with experimental data for single and multiple protuberances will be made.

REFERENCES

1. Polak, A., Werle, M.J., Vatsa, V.N. and Bertke, S.D., "Supersonic Laminar Boundary-Layer Flow Past a Wavy-Wall with Multiple Separation Regions," Rept. AFL 74-12-15, Department of Aerospace Engineering, University of Cincinnati, Cincinnati, Ohio, February 1975. To appear in Journal of Spacecraft and Rockets, 1976.
2. Harris, J.E., "Numerical Solution of the Equations for Compressible Laminar, Transitional and Turbulent Boundary Layers and Comparisons with Experimental Data," NASA TR-R-368, August 1961.

3. Bertke, S.D., Werle, M.J. and Polak, A., "Finite Difference Solutions to the Interacting Supersonic Turbulent Boundary Layer Equations, Including Separation Effects," Rept. AFL 74-4-9, Department of Aerospace Engineering, University of Cincinnati, Cincinnati, Ohio, April 1974.
4. Brandon, H.J., Masek, R.V. and Dunavant, J.C., "Aerodynamic Heating to Corrugation Stiffened Structures in Thick Turbulent Boundary Layers," AIAA Paper No. 75-190, presented at the AIAA 13th Aerospace Sciences Meeting, Pasadena, California, January 20-22, 1975.
5. Shang, J.S. and Hankey, W.L., Jr., "Numerical Solution of the Navier-Stokes Equations for Supersonic Turbulent Flow Over a Compression Corner," AIAA Paper No. 75-3, presented at the AIAA 13th Aerospace Sciences Meeting, Pasadena, California, January 20-22, 1975.
6. Alber, I.E., "Similar Solutions for a Family of Separated Turbulent Boundary Layers," AIAA Paper No. 71-203, presented at the AIAA 9th Aerospace Sciences Meeting, New York, New York, January 25-27, 1971.
7. Davis, R.T., Personal Communication, September, 1975.
8. Blottner, F.G., "Computational Techniques for Boundary Layers," AGARD Lecture Series No. 73, Computational Methods for Inviscid and Viscous Two-and-Three Dimensional Flow Fields, February 1975, pp. 3-1 to 3-51.
9. Dunavant, J.C., Private Communication, August, 1975.
10. Werle, M.J. and Vatsa, V.N., "New Method for Supersonic Boundary Layer Separations," AIAA Journal, Vol. 12, No. 11, November 1974, pp. 1491-1497.

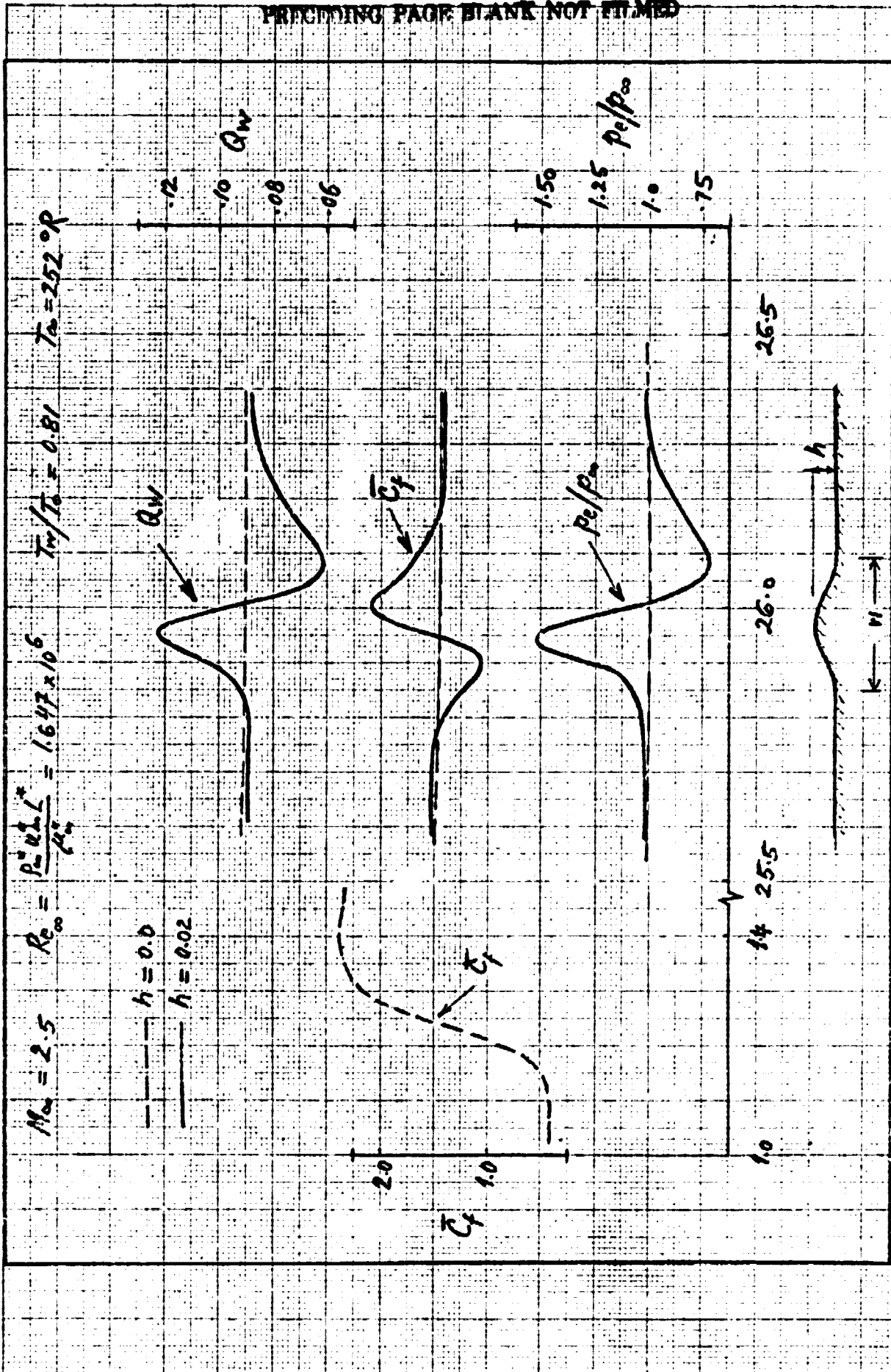


Figure 1. Surface Pressure, Normalized Skin Friction and Heat Transfer - Attached Boundary Layer

$\delta^* = 0.63$ ($\delta^* = \delta L^* = 96 \text{ cm}$); $w^* = WL^* = 3.66 \text{ cm}$; $\delta^* = \delta L^* = 0.305 \text{ cm}$; $C_f = C_f = 0.00144 C_f$;

$$M_\infty = 2.5$$

$$Re_\infty = 1.647 \times 10^6$$

$$Pr = 1$$

$$T_w/T_0 = 1$$

$$T_\infty = 252^\circ R$$

$$h = 0.024$$

$$W = 0.24$$

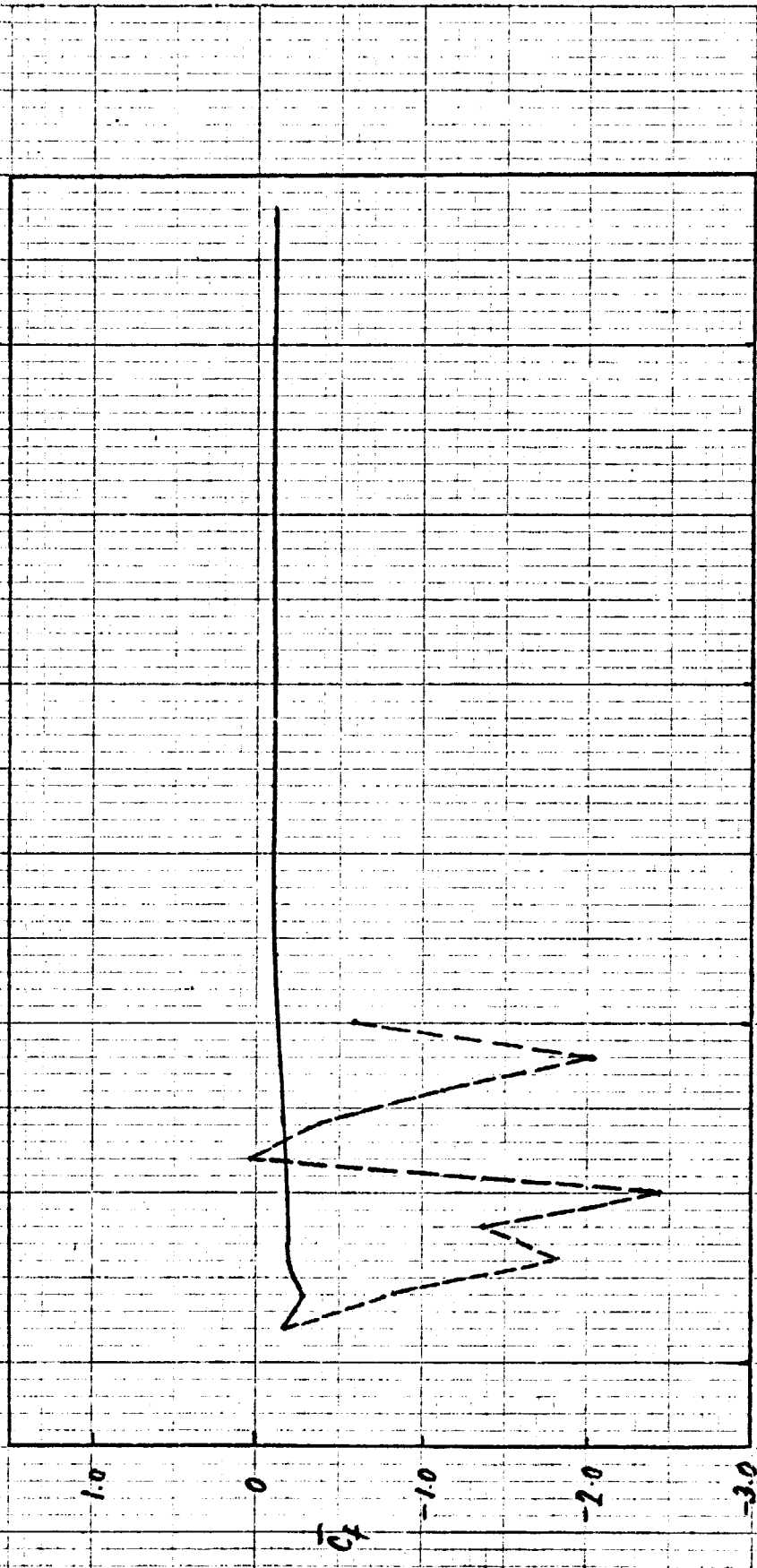


Figure 2. Temporal Variation of Normalized Skin Friction at $s = 3.38$

($t = 7.125$)

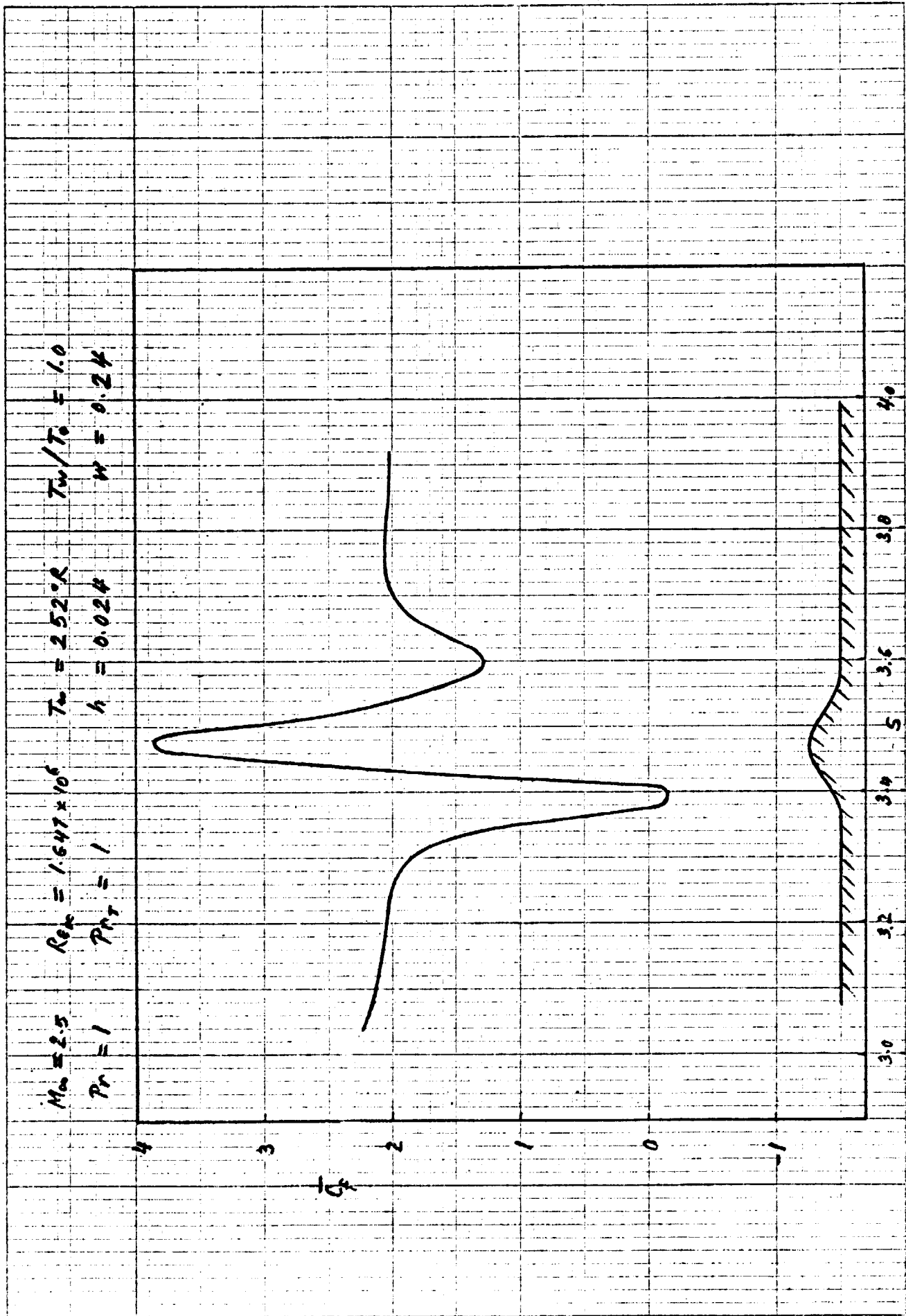


Figure 3. Normalized Skin Friction - Separated Boundary Layer

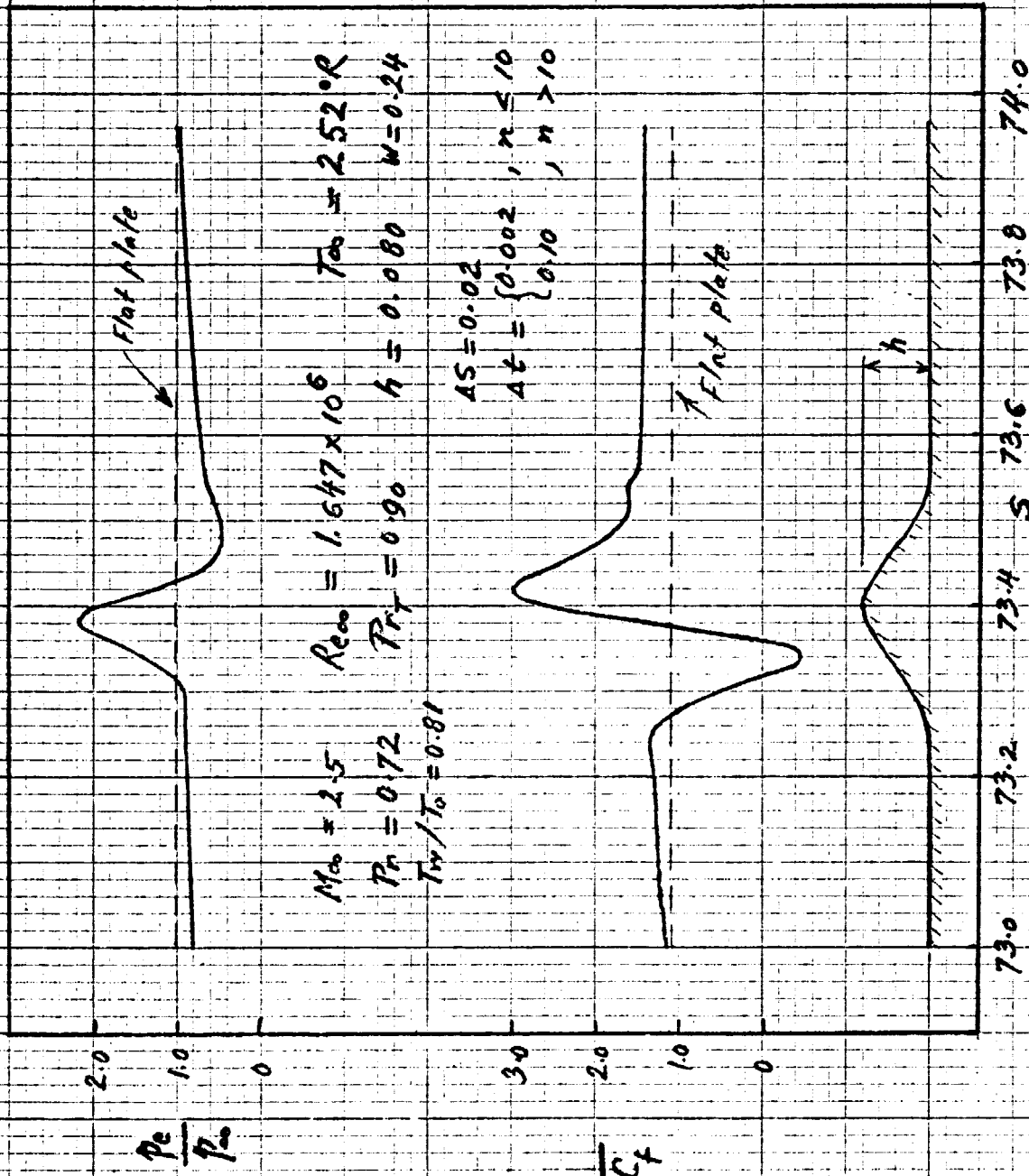


Figure 4. Pressure and Normalized Skin Friction